Trends in Immunotherapy 2024, 8(2), 8925.
https://doi.org/10.24294/ti.v8.i2.8925

Article

Induced tumor associated autoantibodies (iTAAs) by hapten plus drugs for targeting oncogenic nuclear antigens at sentinel lymph node of pancreatic cancer

Lei Wang[1], Baofa Yu[2,3,4,5,*], Jian Zhang[3], Yan Han[3], Guoqin Zheng[2]

[1] Qilu Hospital of Shandong University, Jinan 250012, China
[2] TaiMei Baofa Cancer hospital, Dongping 271500, China
[3] Jinan Baofa Cancer hospital, Jinan 250000, China
[4] Beijing Baofa Cancer Hospital, Beijing 100010, China
[5] Immune Oncology Systems, Inc, San Diego, CA 92102, USA
*** Corresponding author:** Baofa Yu, bfyuchina@126.com

CITATION

Wang L, Yu B, Zhang J, et al. Induced tumor associated autoantibodies (iTAAs) by hapten plus drugs for targeting oncogenic nuclear antigens at sentinel lymph node of pancreatic cancer. Trends in Immunotherapy. 2024; 8(2): 8925. https://doi.org/10.24294/ti.v8.i2.8925

ARTICLE INFO

Received: 2 September 2024
Accepted: 13 September 2024
Available online: 9 October 2024

Abstract: Background: the abscopal is a hypothesis of effect on non-irradiated tumors after localized radiation therapy which associated with the products of tumor-associated gene as autoantibodies (aTAAs) in reaction to the tumor-associated antigens (TAAs). When TAAs interact with hapten within tumor after hapten plus chemotherapy drugs intratumoral injection to pancreatic cancer like tumor lysates vaccine, TAAs-hapten stimulates the immune system as a neu antigen and produces autologous tumor antibodies, it is called induced tumor-associated autoantibodies (iTAAs) which is lightly difference to aTAAs since epitope of antigen linked with hapten. **Method:** immunofluorescence (IF) was applied for detect the binding of the iTAAs in tumor cells at sentinel lymph node. **Results:** aTAAS naturally could not target and bind the TAAs in tumor since due to immune tolerance. The iTAAs can target and bind the TAAS, also the iTAAs targeted in the tumors of sentinel lymph node with complements C help, it was found Cmyc (P = 0.0017 at one week; P = 0.0001 at two weeks), p53 (P = 0.0373; 29.13 ± 6.91, and P = 0.0254), and Zeta (P = 0.1513, P = 0.0044) increased significantly in the tumor cells or perinuclear tumor cells in lymph node at one and two weeks after treatment. Conversely, IMP1 (P = 0.6154; P = 0.0138), Koc (P = 0.5684, P = 0.0103), Survivn (P = 0.1020; P = 0.0147) and Rala (P = 0.3226; P = 0.0249) increased significantly in the cell or perinuclear of tumor in lymph node at two weeks later following. **Conclusions:** it indicated all of iTAAs plays a function in the binding of original cellular tumor genes at sentinel lymph node while the aTAAs could not bind the cellular tumor genes at lymph node due to immune tolerance. We could make a hypothesis: TAAs inside the cancer cells' nuclei can be targeted by the iTAAs which produced by hapten enhanced intratumoral chemotherapy. The iTAA may play a distinctive role in controlling tumor cell growth and resulting in an abscopal effect, which is one of hapten associated with TAA induced immune response.

Keywords: tumor associate antigen (TAA); tumor-associated autoantibodies (TAA) induced autologous tumor antibodies (iATA); neu antigens; hapten; hapten induced immunotherapy

1. Introduction

The supraclavicular lymph node is an outpost indicating tumor metastasis, which can be easily detected by palpation or surgical removal for examination of pathological, tumor sourcing. The presence of enlarged lymph nodes may indicate tumor metastasis and immunity reaction by the stimulation of any immunological related antigen or therapy. These newly formed cells generate a humoral immune

response in their relative microenvironment, like the lymph node [1,2]. The supraclavicular lymph node is a common place of metastasis for patients with pancreatic adenocarcinoma and indicates advantage of disease into the stages III to IV [3].

However, as cancer occurrences or progresses, the amplification of tumor-associated autoantibodies (aTAAs) in response to natural tumor-associated antigens (TAAs) appears a promising early diagnostic biomarker of cancerous cells [4]. This phenomenon was further confirmed by researchers who used aTAAs combined miRNAs to examine esophageal squamous cell carcinoma (ESCC) [5,6]. A previous study demonstrated that TAAs can stimulate the immune system to produce autologous tumor antibodies, which induced by hapten enhanced intratumoral chemotherapy related with B cell immunity (HEIC) [7,8]. HEIC is a method of chemo drug kill tumor and can further trigger the release of damage-associated molecular patterns (DAMPs) and antigens from dying tumor cells, which is modified by hapten to be neuTAAs within tumor to activate the innate immune response, HEIC is also like the tumor lysate vaccine to induce immune response, especially whole cancer cells or cancer cell lysates, it is a very promising approach associated with T cell immunity [9–11]. A phase I study was showing a promise with allogeneic tumour cell lysate induce tumour-reactive T-cell responses in patients with pancreatic cancer [12]. These newly formed antibodies of TAA as representative genes (P53, Zeta, IMP1, Koc, Survivn) associated with B-cell immunity is called an induced tumor autologous antibodies or induced tumor-associated antibodies (iTAAs), which is lightly difference to aTAAs naturally formed since epitope of antigen linked with hapten [8].

Reported aTAAs as biomarkers for detection predominantly relate to the occurrence and recovery of tumors [13–15]. However, the iTAAs share a connection with immunotherapy for cancer since iTAAs may have higher specificity due to their epitope of TAA linked with hapten, and iTAAs may play a role of binding the TAAs [7,8,16]. Until now, little has been known about the location of iTAAs final to be and whether iTAAs can enter tumor cells and weather it needs to associate with the complement response.

In addition, we aimed to decipher if the interdependence of tumor cell membranes is an adjuvant function and if the iTAAs travel to metastasized tumor cells in the sentinel lymph node. This focus was set to advance our understanding of the relationship between iTAA can target tumor nuclear antigen at site of metastasis after HEIC like the tumor lysate vaccine, produce an immune response for control tumor growth.

2. Materials and method

Clinical Specimens: three patients had a definite clinical diagnosis of pancreatic cancer with pathological adenocarcinoma at Peking Union Medical College Hospital. Patients also met the indications for hapten enhanced intratumoral chemoimmunotherapy (HEIC) and signed the informed consent form (**Table 1**). This experiment was approved by the ethics committee of Taimei Baofa Cancer Hospital hospital (TMBF 0010, 2015), and all methods for experiments were performed

following relevant guidelines and regulations.

Table 1. iTAA measured in blood circulation before and after treatment.

Time / Name genes	Before treatment	One week after treatment
Koc	0.074	0.182
Survivin	0.057	0.073
IPM1	0.072	0.103
Zeta	0.080	0.203

Note: TAAs' levels (μg/mL) at before and after treatment.

Patients received 8 mL intratumoral injection at the pancreatic location under CT guidance, constituent of 1.00 mg/mL doxorubicin hydrochloride (Dox), 0.80 mg/mL of cytarabine (Ara-C), 20.0 mg/mL of H_2O_2 and 144 mg/mL of penicillin [7,8,11]. Surgical biopsy samples were collected from a supraclavicular lymph node for the patients three times before and one to two weeks after HEIC treated pancreatic tumor site for immunohistochemical staining. Meanwhile patients' blood was taken for analysis of autologous antibodies (iTAA) before and two weeks following treatment.

Antibody Detection Analysis: An enzyme-linked immunosorbent assay (ELISA) was used to dilute four purified recombinant proteins of TAA as representative genes (Zeta, IMP1, Koc, Survivn) in phosphate-buffered saline (PBS) from 0.125 ug/mL to 1.0 ug/mL. The proteins were then coated in a 96-well microliter plate (100 uL/well) overnight at 4 ℃ and incubated in a 1:200 diluted serum in antigen-coated wells (100 uL/well) for 90 min at room temperature (RT). The proteins were then incubated in a 1:3000 dilution of horseradish peroxidase-conjugated goat anti-human IgG [9,10].

A 2,2'-azidobis-3-ethylbenzothiazoline-6-sulfonic acid (ABTS) substrate. Then 100 uL of hydrogen peroxide was added to each well. The plates were incubated without light for 10 to 15 min at RT. Each well's optical density (OD) value was immediately read at 405 nm on the Varioskan LUX Multimode Microplate Reader to reduce the plates' variation [13]. Subsequently, two blank controls of 1% BSA in PBST and 8 frozen human serum samples were administered to each well of all 96-well plates. This step allowed for the normalization of different plates' OD values and adjustment of the background of all plates used [9,10].

Reagents for IF Staining: complement C3 (excitation wavelength, Ex: 652 nm, Em: 668 nm, red), C5 (Ex: 495 nm, Em: 519 nm, green), and C9 (Ex: 555 nm, Em: 565 nm, red) kits were purchased from Abcam. The zeta, IMP1, Koc, Survivn, c-MYC, RalA, and p53 TAAs were synthesized with fluorescence by Beijing Yiqiao Shenzhou Technology Co., Ltd. (Em: 540 nm, green). After these samples were taken, they were immediately preserved in formalin, embedded in paraffin, and sectioned. Complement C and Zeta, IMP1, Koc, Survivn, c-MYC, RalA, and p53 TAA-bearing fluorescein staining were performed to observe the differences in the staining of complement C3, C5, and C9 versus the Zeta, IMP1, Koc, Survivn, c-MYC, RalA, and p53 iTAAs in different slides of tumor tissues before and after treatment (See Appendix).

IF Staining-Complement: Complements staining was conducted to observe the differences in the reaction staining of complement C3, C5, and C9 before and after treatment. The procedure was performed via the several steps [8,14].

IF Staining-TAA: TAA-bearing fluorescein staining was executed to depict the target binding of zeta, IMP1, Koc, Survivn, c-MYC, RalA, and p53 iTAAs in different tumor tissues. The procedure went as such previous study, mounted the slides with an anti-fluorescence quencher and stored them at 4 ℃ (see Appendix) [8,14].

IF-Imaging and Analysis: After staining was complete, each section was photographed at Shandong University with a multi-spectral panoramic tissue scanning microscope (TissueFAXS Spectra). An individual blinded to this study and had no conflict of interest performed this photograph and then conducted fluorescence imaging and data analysis. Equation (1) [8,14].

$$\text{Positive cell rate (Cell \%)} = \left[(\#\text{of tumor} - \text{related autoimmune antibody}) - \left(\text{positive}\frac{\text{cells}}{\text{total}}\#\text{ of cells}\right)\right] \times 100\% \quad (1)$$

Statistical Analysis: Each microscopic field from one slide of pathological tissue acted as an independent cell population. There is six individual cell population from each pathological slide. The expression differences of complement C3, C5, and C9, as well as the zeta, IMP1, Koc, Survivn, c-MYC, RalA, and p53 iTAAs from the six population of the slides in the tissues, were analyzed before and after treatment using GraphPad Prism v8.0.2.263 [8,14]. A paired t-test was used to determine the percentage of positive cells and immunofluorescence intensity (MFI), and $P < 0.05$ indicated a statistically significant difference.

3. Results

Antibody Detection Analysis: The blood detection has confirmed that the level of four of iTAA increased significantly after HEIC treatment than that before treatment. It indicated that hapten with TAA could induce the tumor associate antibody (iTAA) response to the stimulate of tumor antigens linked hapten in tumor death by HEIC, it has shown that iTAA was induced and increased than earlier time (**Tables 1** and **2**).

Cell population was selected for analysis: Cell population was selected under scanning microscope from six fields of each slide for each patient as general number of calculation from total 15 slides before and after HEIC, these cell included T cells, B cells, mononuclear phagocytes and stromal cells, mast cells, neutrophils, pDCs, epithelial cells, etc., cells distribution is difference compared with that before (1) and one, (2) and two weeks, (3) after HEIC form selection of six population, the distribution C3: (1) the positive cells is 193, 1.83% of 10527 total cells, (2) the positive cells is 1188, 30.48% of 3897 total cells, (3) the positive cells is 207, 20.6% of 1005 the total cells; C5: (1) the positive cells is 8582, 72.83% of 11784 total cells, (2)the positive cells is 3459, 95.08% of 3638 total cells, (3) the positive cells is 1290, 88.05% of 1465 total cells; C9: (1) the positive cells is 1447, 10.34% of 13995 total cells, (2) the positive cells is 2537, 47.91% of 5295 total cells, (3) the positive cells is 544, 27.3% of 1993 total cells, it indicated that C3, C5 and C9 may bind the

difference type of cells at difference ratio, C3 and C9 has more selectivity biding (**Table 2**).

Table 2. Comparison of positive expression percentage of pancreatic cancer lymphatic metastasis before and after treatment by fluorescence staining (Mean ± SEM).

Kind of genes and complement		Cell positive ratio (%)			[1]P	[2]P
		Before therapy	1 week after therapy	2 weeks after therapy		
C3	Cell+ %	2.03 ± 0.59	34.09 ± 8.77	18.85 ± 6.01	0.0204	0.0405
	MFI	18.50 ± 1.04	40.89 ± 5.90	29.98 ± 3.73	0.0322	0.2323
C5	Cell+ %	72.96 ± 8.18	95.60 ± 0.97	87.26 ± 3.09	0.0088	0.2717
	MFI	40.37 ± 5.90	57.44 ± 4.62	46.28 ± 2.07	0.0058	0.1742
C9	Cell+ %	10.64 ± 3.04	47.30 ± 5.42	28.14 ± 12.80	0.0146	0.2865
	MFI	24.12 ± 2.03	45.18 ± 3.91	31.71 ± 7.72	0.5684	0.0103
Cmyc	Cell+ %	11.39 ± 4.00	17.42 ± 6.68	54.90 ± 10.21	0.0017	0.0001
	MFI	7.71 ± 1.35	10.26 ± 4.39	32.88 ± 8.12	0.0069	0.0001
Koc	Cell+ %	3.86 ± 0.90	20.65 ± 7.64	17.82 ± 4.02	0.5684	0.0103
	MFI	5.15 ± 045	11.39 ± 3.83	9.59 ± 1.74	0.6493	0.0292
Survivn	Cell+ %	8.75 ± 2.26	14.86 ± 5.93	40.71 ± 7.29	0.1020	0.0147
	MFI	7.61 ± 0.57	8.67 ± 2.47	18.33 ± 2.72	0.0326	0.0243
p53	Cell+ %	3.79 ± 2.76	36.86 ± 9.57	29.13 ± 6.91	0.0373	0.0254
	MFI	3.50 ± 1.29	18.35 ± 4.65	14.11 ± 2.78	0.2034	0.0120
IMP1	Cell+ %	1.89 ± 0.61	28.35 ± 10.65	27.47 ± 7.98	0.6154	0.0138
	MFI	4.00 ± 0.67	13.86 ± 4.60	13.56 ± 2.85	0.0621	0.0280
Rala	Cell+ %	15.29 ± 5.36	56.81 ± 6.84	78.08 ± 5.91	0.1022	0.0324
	MFI	12.33 ± 1.35	28.12 ± 4.11	34.32 ± 2.79	0.1513	0.0044
Zeta	Cell+ %	5.07 ± 1.86	16.80 ± 6.76	29.23 ± 8.77	0.3226	0.0249
	MFI	5.91 ± 0.82	9.29 ± 2.51	13.38 ± 3.07	0.0176	0.0441

Note: [1]P: 1 week after treatment vs. before treatment. [2]P: 1 week after treatment vs before treatment.

The TAA binding distribute is different before (1) and one (2) and two weeks (3) after HEIC with more selectivity to tumor cells, Cmyc: (1) the positive cells is 534, 12.01% of 4445 total cells, (2) the positive cells is 662, 24.09% of 2748 total cells, (3) the positive cells is 1328, 62.64% of 2120 total cells, Koc: (1) the positive cells is 126, 3.56% of 3535 total cells, (2) the positive cells is 836, 23.97% of 3488total cells, (3) the positive cells is 179, 16.78% of 1067 total cells; Survivn: (1) the positive cells is 165, 6.92% of 2384 total cells, (2) the positive cells is 476, 16.15% of 2947 total cells, (3) the positive cells is 611, 41.42% of 1475total cells; p53:(1) the positive cells is 225, 4.57% of 4923 total cells, (2) the positive cells is 1546, 39.13% of 3951 total cells, (3) the positive cells is 438, 33.03% of 1326 total cells; IMP1: (1) the positive cells is 68, 1.92% of 3533 total cells, (2) the positive cells is 926, 37.25% of 2486 total cell, (3) the positive cells is 336, 32.06% of 1048 total cells; Rala: (1) the positive cells are 123, 14.64% of 840 total cells, (2) the positive cells are 1580, 56.75% of 2784 total cells, (3) the positive cells are 750, 74.26% of 1010 total cells; Zeta: (1) the positive is 231, 5.53% of 4174 total cells,

(2) the positive cells are 416, 18.42% of 2258 total cells, (3) the positive cells are 401, 34.24% of 1171 total cells. It indicated that TAA binds to the tumor cell more selectively, and the binding percentage at one or two weeks after HEIC is higher than before treatment, and the binding percentage at two weeks after HEIC is higher than that of one week (**Table 2**).

Positive Complement Cells and iTAAs' Mean Immunofluorescence Intensity (MFI) Rates: Before and after treatment, analysis of the positive staining of the complement, the iTAAs, and mean immunofluorescence intensity (MFIs) were executed for each factor in all tumor sections. The percentage of the positive complement was higher after than before for complement, C3 (2.03 ± 0.59 vs. 34.09 ± 8.77, $P < 0.0204$, 18.85 ± 6.01, $P < 0.0405$) (**Table 2**, **Figure 1A,B**, **Figure 2A**: B1 and B2), C5 (72.96 ± 8.18 vs. 95.60 ± 0.97, $P < 0.0088$; 87.2 ± 3.09, $P < 0.2717$) (**Table 2**, **Figure 1A,B**, **Figure 2B**: A, B1 and B2), C9 (10.64 ± 3.04 vs. 47.30 ± 5.42, $P < 0.0146$; vs. 28.14 ± 12.80, $P < 0.2865$) (**Table 2**, **Figure 1A,B**, **Figure 2C**: A, B1 and B2). The percentage of the positive complement was higher after than before for TAAs, Cmyc (11.39 ± 4.00 vs. 17.42 ± 6.68, $P < 0.0017$; vs. 54 ± 10.21, $P < 0.0001$) (**Table 2**, **Figure 1A,B**, **Figure 3A**: A, B1 and B2); IMP1 (1.89 ± 0.61 vs. 28.35 ± 10.65, $P < 0.6154$; vs. 27.47 ± 7.98, $P < 0.0138$) (**Tables 1** and **2**, **Figure 1A,B**, **Figure 3B**: A, B1 and B2), Koc (7.71 ± 1.35 vs. 10.2 ± 4.39, $P < 0.5684$, vs. 32.88 ± 8.12, $P < 0.0103$) (**Table 2**, **Figure 1A,B**, **Figure 3C**: A, B1 and B2), P53 (3.79 ± 2.76 vs. 36.86 ± 9.57, $P < 0.0373$; vs. 29.13 ± 6.91, $P < 0.0254$) (**Table 2**, **Figure 1A,B**, **Figure 3D**: A, B1 and B2), Rala (15.29 ± 5.36 vs. 56.81 ± 6.84, $P < 0.1022$; vs.78.08 ± 5.91, $P < 0.0324$) (**Table 2**, **Figure 1A,B**, **Figure 3E**: A, B1 and B2), Survivn (8.75 ± 2.26 vs. 14.86 ± 5.93, $P < 0.1020$; vs. 40.71 ± 7.29, $P < 0.0147$) (**Table 2**, **Figure 1AB**, **Figure 3F**: A, B1 and B2), Zeta (5.07 ± 1.86 vs. 16.80 ± 6.76, $P < 0.3226$; vs. 29.23 ± 8.77, $P < 0.0249$) (**Table 2**, **Figure 1A,B**, **Figure 3G**: A, B1 and B2). This finding illustrates that after patients' bodies produced the iTAAs, the iTAAs target to bind the tumor cells and tumor cells' nuclei at the sentinel lymph node of pancreatic cancer.

The MFI was significantly higher after versus before HEIC for the complement, C3 (18.50 ± 1.04 vs. 40.89 ± 5.90, $P < 0.2323$; vs. 29.98 ± 3.73, $P < 0.0322$) (**Table 2**, **Figure 1A,B**, **Figure 2A**: A, B1 and B2), C5 (40.37 ± 5.90 vs. 57.44 ± 4.62, $P < 0.0058$, vs. 46.28 ± 2.07, $P < 0.1742$) (**Table 2**, **Figure 2B**: A, B1 and B2), C9 (24.12 ± 2.03 vs. 45.18 ± 3.91, $P < 0.5684$; vs. 31.71 ± 7.72 → 0.5684, $P < 0.0103$) (**Table 2**, **Figure 2C**: A, B1 and B2). The MFI was significantly higher after versus before hapten-enhanced chemotherapy for TAAs, Cmyc (7.71 ± 1.35 vs. 10.26 ± 4.39, $P < 0.0069$; vs. 32.88 ± 8.12, $P < 0.0001$) (**Table 2**, **Figure 1**, **Figure 3A**: A, B1 and B2), IMP1 (4.00 ± 0.67 vs. 13.86 ± 4.60, $P < 0.0621$; vs.13.56 ± 2.85, $P < 0.0280$) (**Table 2**, **Figure 1**, **Figure 3B**: A, B1 and B2), Koc (5.15 ± 045 vs. 11.39 ± 3.83, $P < 0.6493$; vs. 9.59 ± 1.74, $P < 0.0292$) (**Table 2**, **Figure 1**, **Figure 3C**: A, B1 and B2), P53 (3.50 ± 1.29 vs. 18.35 ± 4.65, $P < 0.2034$; vs.14.11 ± 2.78, $P < 0.0120$) (**Table 2**, **Figure 1**, **Figure 3D**: A, B1 and B2), Rala (12.33 ± 1.35 vs. 28.12 ± 4.11, $P < 0.1513$, vs.34.32 ± 2.79, $P < 0.0044$) (**Table 2**, **Figure 1**, **Figure 3E**: A, B1 and B2), Survivn (7.61 ± 0.57 vs. 8.67 ± 2.47, $P < 0.0326$; vs. 18.33 ± 2.72, $P < 0.0243$) (**Table 2**, **Figure 1**, **Figure 3F**: A, B1 and B2), Zeta (5.91 ± 0.82 vs. 9.29 ± 2.51, $P < 0.0176$; vs. 13.38 ± 3.07, $P < 0.0441$) (**Table 2**, **Figure 1**, **Figure 3G**: A, B1 and B2).

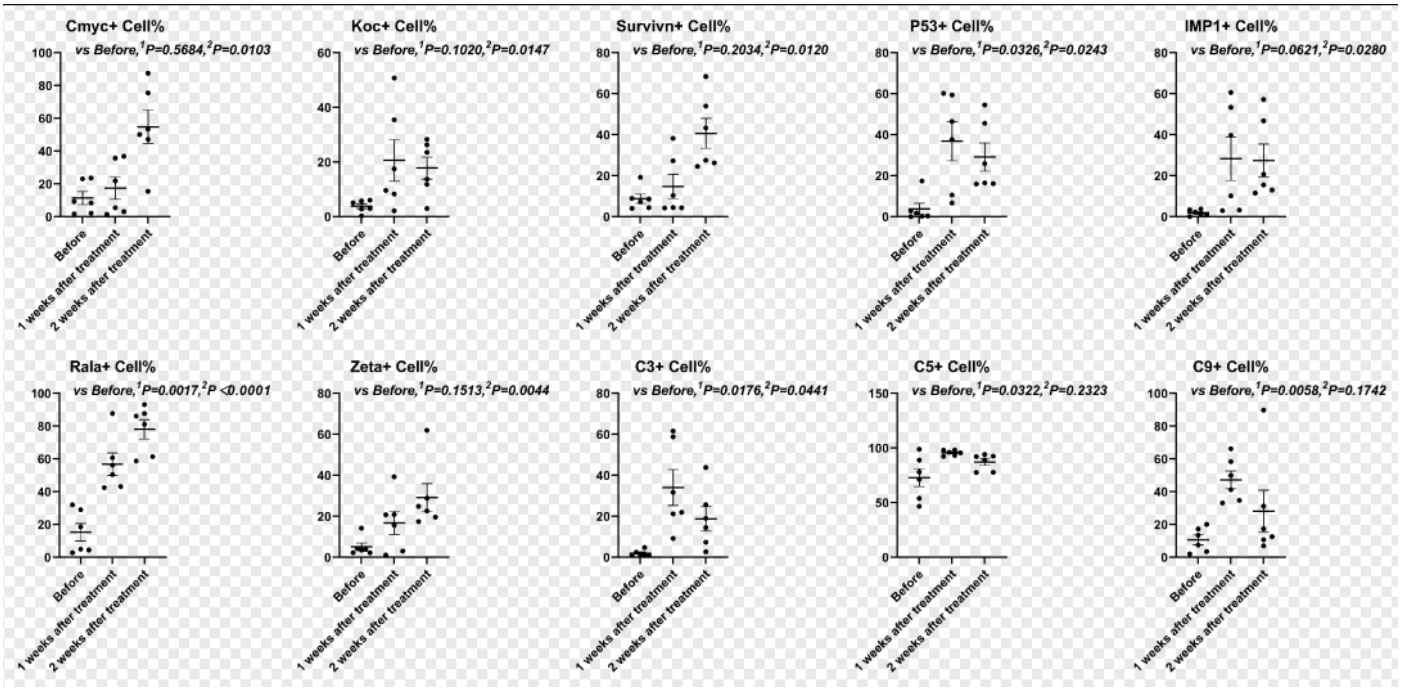

(A)

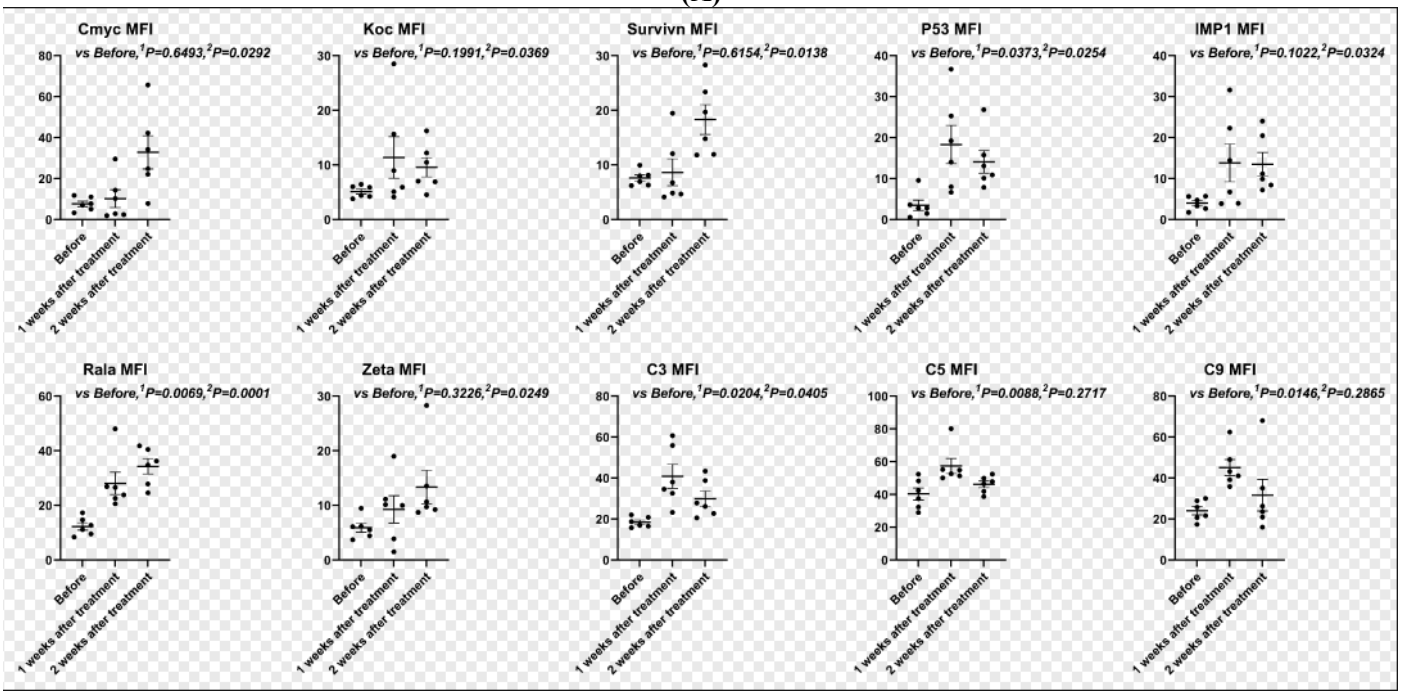

(B)

Figure 1. (A) Tumor genes and complement positive reaction and target binding rate of tumor-related immune autoantibody positive cells before and after HEIC treatment; **(B)** mean immunofluorescence intensity (MFI) of complement (C3, C5 and C9) and tumor-associated immune autoantibodies before and after HEIC treatment.

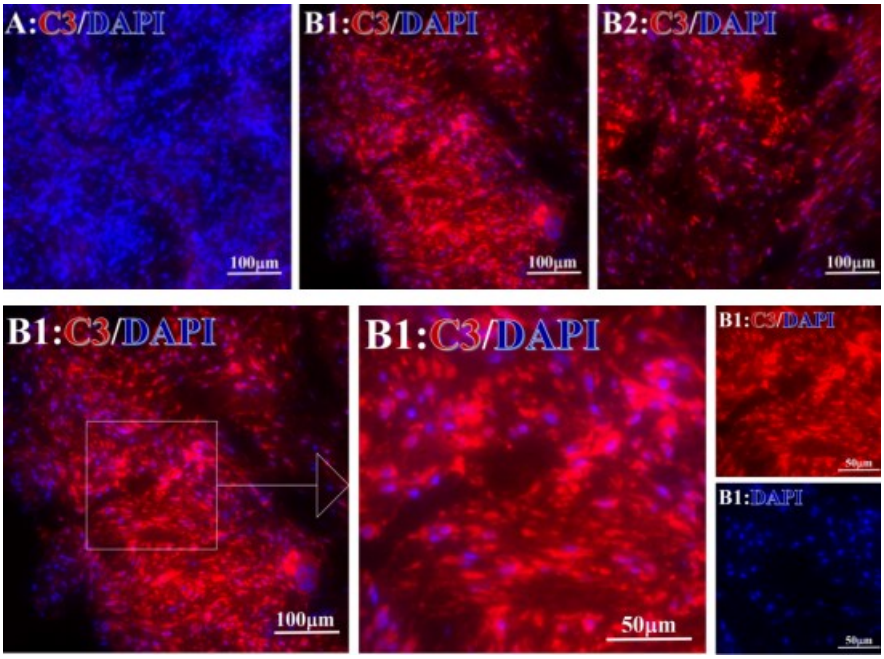

(A)

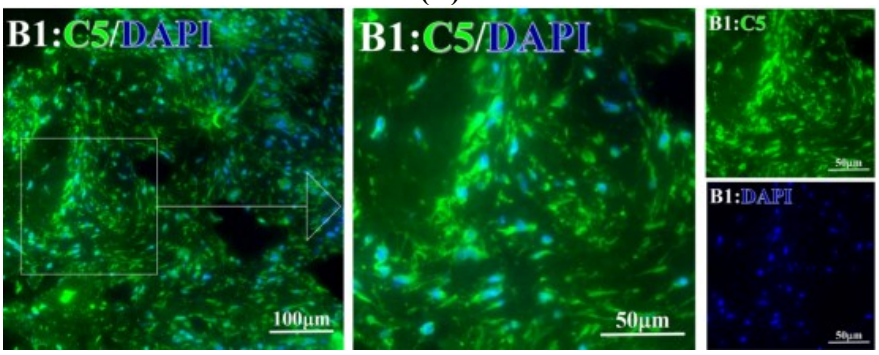

(B)

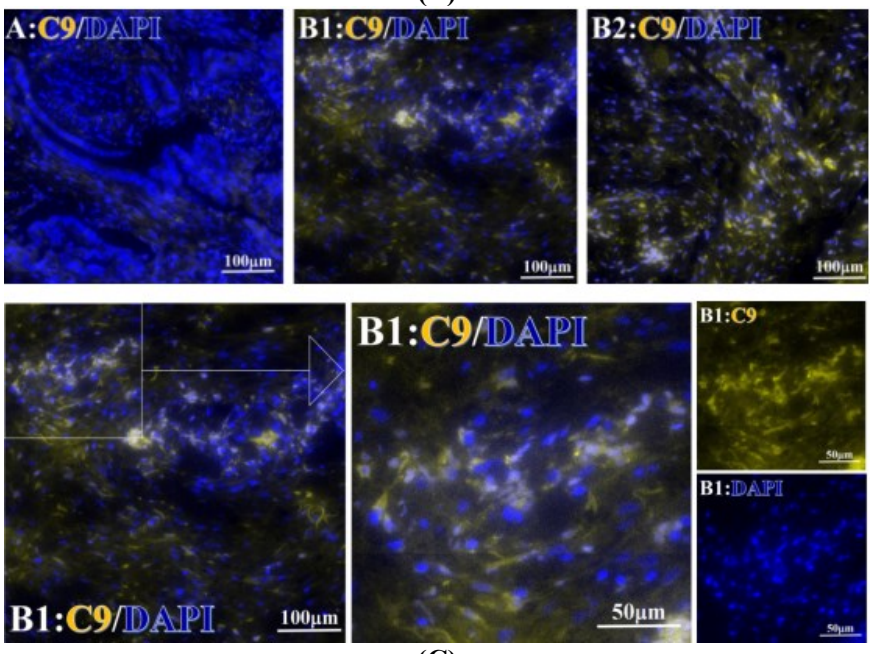

(C)

Figure 2. (A) Example graph of C3 fluorescence reaction before and after HEIC treatment; **(B)** example graph of C5 fluorescence reaction before and after primary tumor HEIC treatment; **(C)** example graph of C9 fluorescence reaction before and after primary tumor HEIC treatment.

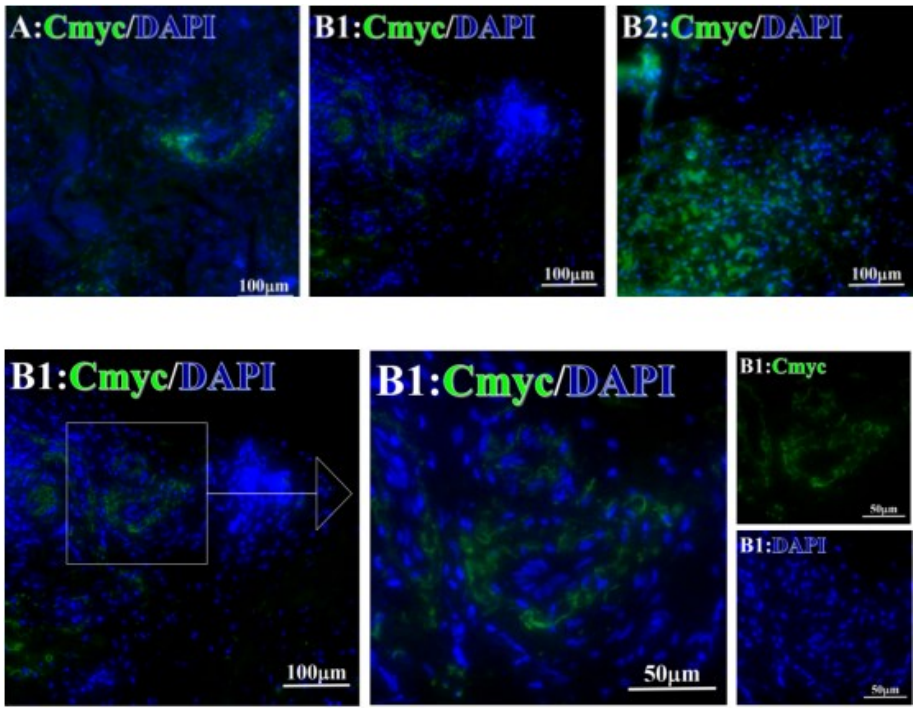
A:Cmyc/DAPI
B1:Cmyc/DAPI
B2:Cmyc/DAPI
100μm
B1:Cmyc/DAPI
B1:Cmyc/DAPI
B1:Cmyc
B1:DAPI
50μm

(A)

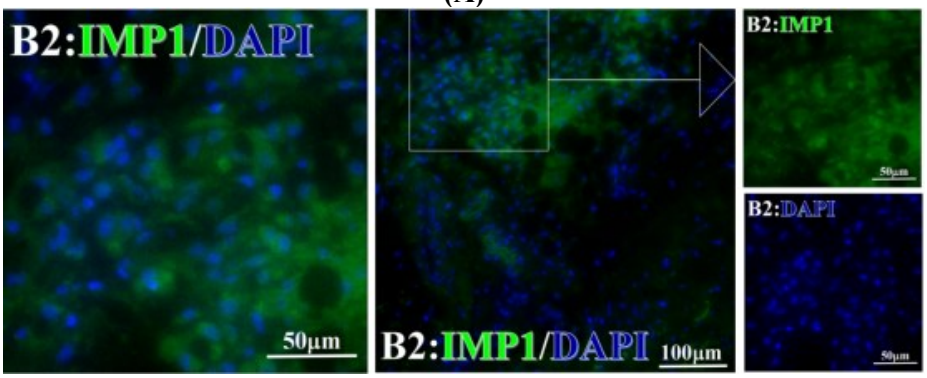
B2:IMP1/DAPI
B2:IMP1/DAPI
B2:IMP1
B2:DAPI
50μm
100μm

(B)

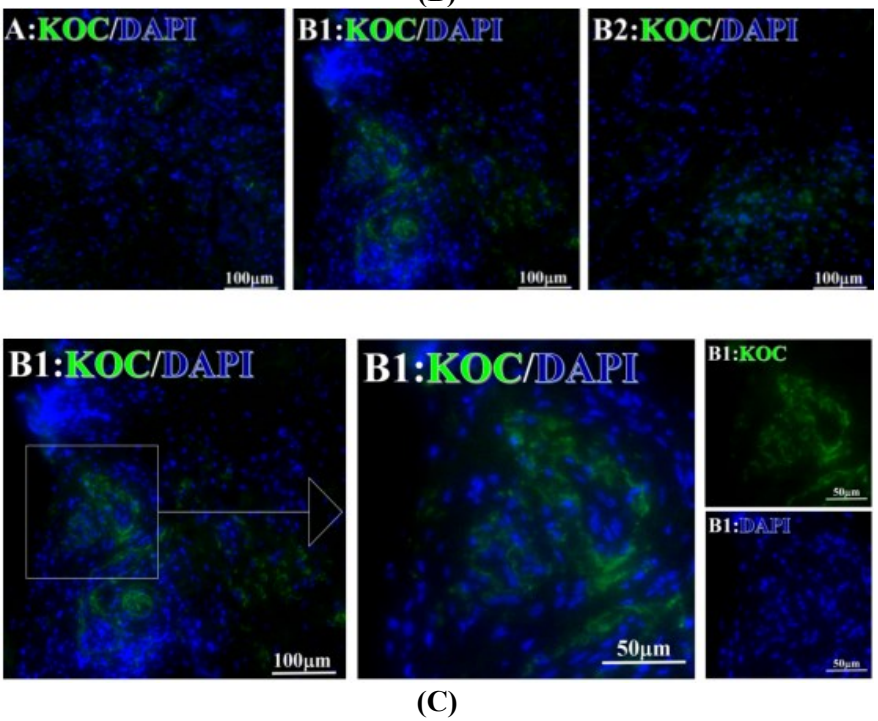
A:KOC/DAPI
B1:KOC/DAPI
B2:KOC/DAPI
100μm
B1:KOC/DAPI
B1:KOC/DAPI
B1:KOC
B1:DAPI
50μm

(C)

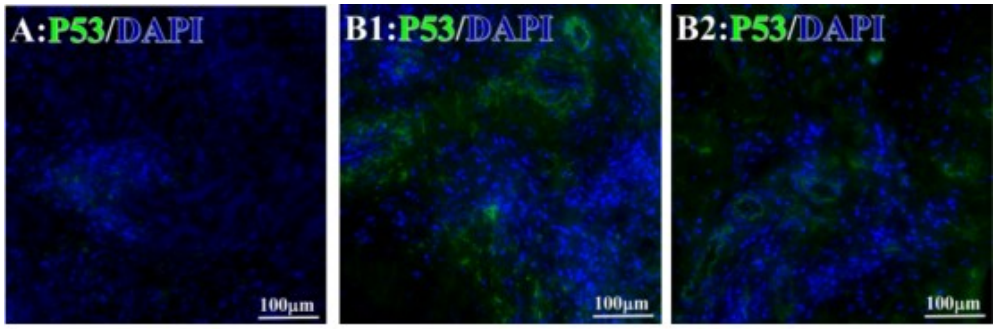
A:P53/DAPI
100μm
B1:P53/DAPI
100μm
B2:P53/DAPI
100μm

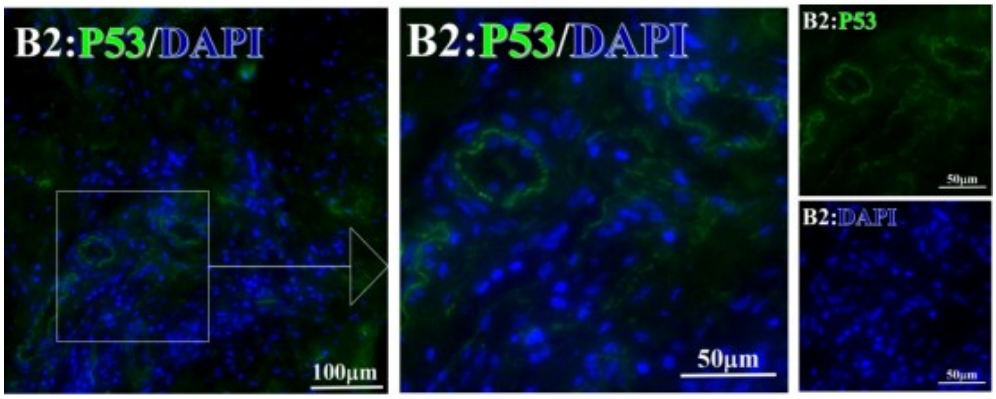
B2:P53/DAPI
100μm
B2:P53/DAPI
50μm
B2:P53
50μm
B2:DAPI
50μm

(D)

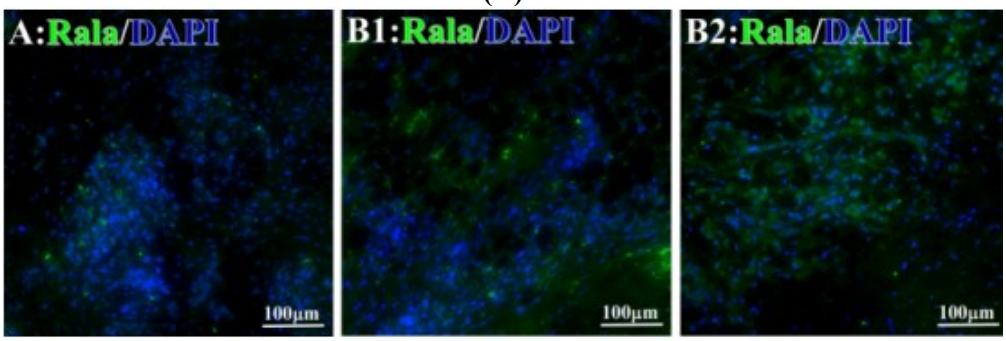
A:Rala/DAPI
100μm
B1:Rala/DAPI
100μm
B2:Rala/DAPI
100μm

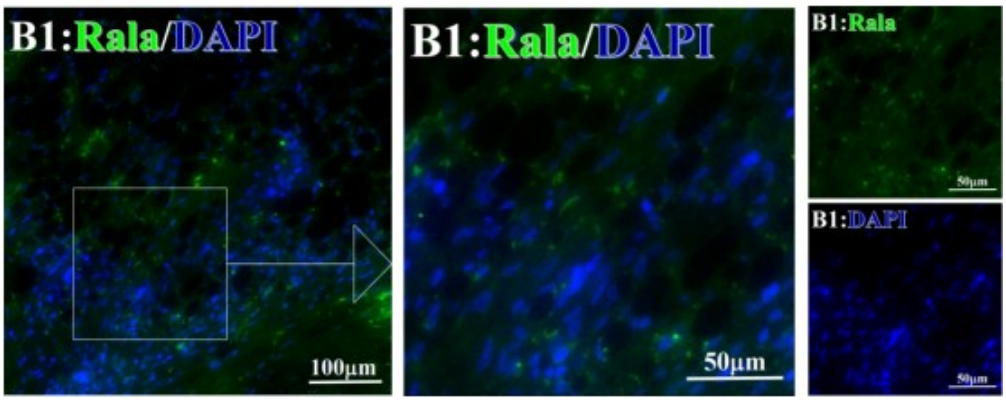
B1:Rala/DAPI
100μm
B1:Rala/DAPI
50μm
B1:Rala
50μm
B1:DAPI
50μm

(E)

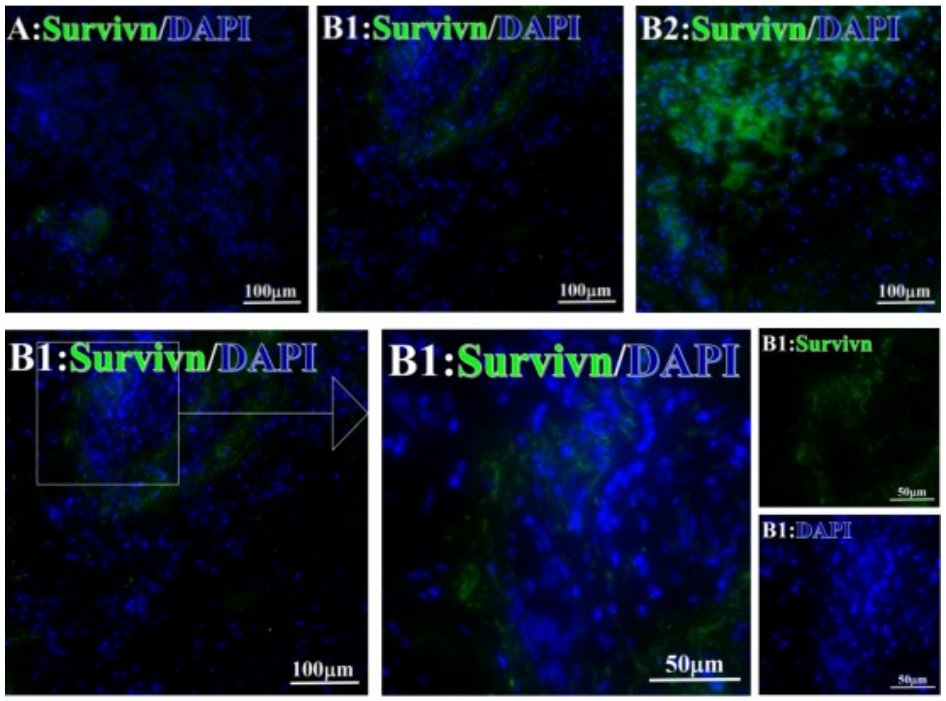

(F)

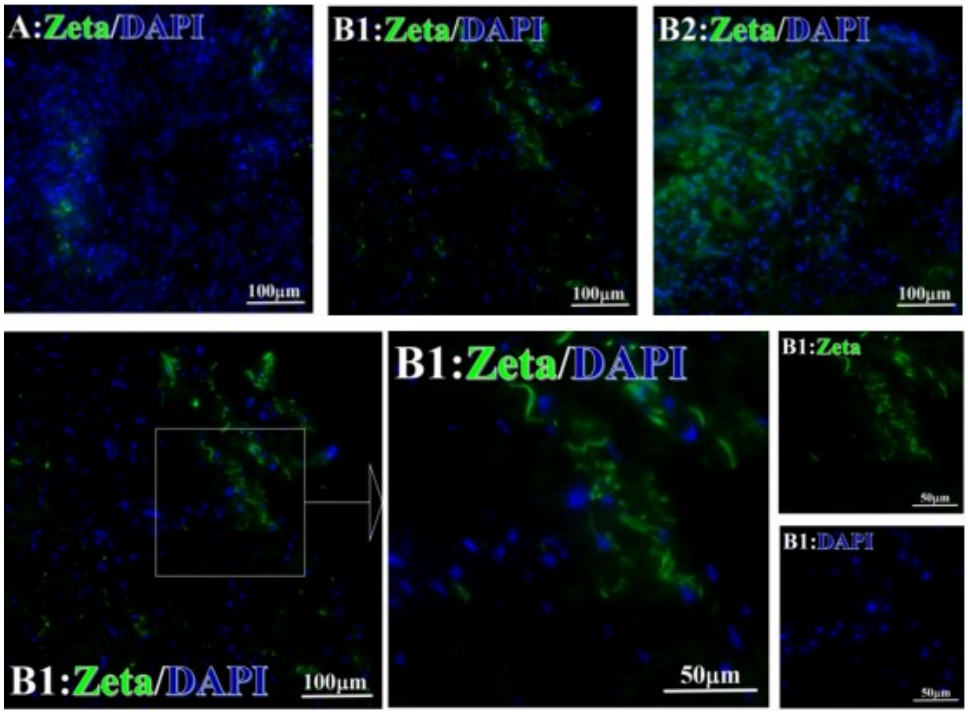

(G)

Figure 3. (A) Examples iTAA of Cmyc fluorescence target binding positive cells before and after primary tumor HEIC treatment; **(B)** example map of target binding position for iTAA of IMP1-positive cells before and after primary HEIC treatment; **(C)** examples iTAA of KOC fluorescence target binding positive cells before and after primary HEIC treatment; **(D)** examples iTAA of P53 fluorescence target binding positive cells before and after primary HEIC treatment; **(E)** examples iTAA of Rala fluorescence target binding positive cells before and after primary HEIC; **(F)** examples iTAA of Survivn fluorescence target binding positive cells before and after primary HEIC treatment; **(G)** examples iTAA of Zeta fluorescence target binding positive cells before and after primary HEIC treatment.

4. Discussion

aTAAs are commonly produced in the human body and maintain a low-level presence and the level of aTAAs may soar if a mutation happens in the genes of TAAs by virus for an unknown reason [4,17]. The mutation can occur when viruses or mutated proteins of oncogenes or suppress genes other than those originating from the human body cause tumors [4,17]. An antibody's amplification response to the presence of an antigen, it means that even a small quantity of antigens in the early stage of tumorigenesis can trigger a relatively large immune response [18]. Therefore, aTAAs are feasible as early diagnostic markers of pancreatic adenocarcinoma too. aTAAs as biomarkers natural produced, it is slight difference from iTAAs which induced thorough HEIC like tumor lysates vaccine, it should be further studied in detail [8].

We have established that HEIC can induce an immune response, it showed tumors with CD4 and CD8 positive tumor tissue and the DC11b/c expression was increased in tumor in mice model due to hapten modified TAAs or epitope of TAA linked with hapten [19]. Therefore, it is confirmed iTAA of Koc, Survivin. IPM1and Zeta in the blood (**Table 1**) and tumor tissue section were a higher level at one and two weeks after HEEIC (**Table 2**). After the iTAAs' activated production, iTAAs circulate and look the target, then bind to tumor cells at the tumor cells. Thus, this study has confirmed that the iTAAs can be induced and excited in the patient body while T-cell function may induce following HEIC treatment [7], and iTAA can bind to the tumor metastasis in the sentinel lymph node (**Figures 1** and **3**). This study also has confirmed that the complements C3, C5, and C9 are primarily located in the perinuclear region of tumor cells and other cells (**Table 2**, **Figure 2**). The C3 and C9 reactions on the surface of tumor cells may active to punch holes of cell membrane for iTAA enter the intranuclear region of tumor cells. This study is the first to use IF with different tumor antigen-bearing fluorescence to detect the iTAAs of TAAs in the tumor of sentinel lymph nodes. Typically, this process is used to test the blood level of autoantibodies of TAAs as biomarkers for diagnosis [17].

Since the iTAAs was not found in the patient's tumor cells of sentinel lymph nodes before HEIC treatment, it may further confirm emerges supporting the assertion that the iTAAs is more specific to TAA than TAA natural, so that iTAAs increase in sentinel lymph nodes following HEIC treatment and metastasis is a critical target location for iTAAs (**Table 2**), the HEIC action like tumor lysate vaccine, this may be molecular evidence for immune response which involved in the abscopal effect. iTAA of four iTAAs was confirmed to have significantly higher in the blood after HEIC treatment (**Table 1**). The staining iTAAs of Cmyc, p53, and zeta increased significantly in the tumor cell or perinuclear of tumor cell locations at one and two weeks following HEIC treatment. Conversely, the expressions of IMP1, Koc, Survivn, and Rala were significantly increased in the tumor cell or perinuclear of tumor cell locations at two weeks after HEIC (**Table 2**). Irrespective of the timing, all of iTAA could be action any time, the target binding rate revealed that different iTAA could bind to different original cellular position in tumor cells at any location of tumor metastasis, not restricted to the sentinel lymph node of metastasis, which could play a unique role in the regulation of tumor cell growth with complement

associates (**Tables 1** and **2**). The seven iTAAs are only representative of countless tumor gene products, the sentinel lymph node is just a representative of countless lymph nodes in the whole body.

Since the iTAAs were monitored at sites of metastasis where HEIC was not preformed, treated only at site of pancreatic cancer, it is further confirmed that iTAA has been induced, spilled in circulation (**Table 1**), and located tumor cells nuclei in the sentinel lymph node (**Table 2**). Additionally, our results establish that once induced, iTAAs could circulate in the blood to search for the primary tumor or metastasis site to bind the cell or nuclei of those tumor which may related to immune response as abscopal effect [18].

In shortly, hapten-enhanced intra-tumoral injections into tumor in patients as tumor lysates vaccine, it can induce the iTTAs during to haptenation with TAAs within tumor after HEIC, more studies are required to develop a comprehensive understanding of the full therapeutic potential of the iTTAs.

Author contributions: Conceptualization, BY; methodology, JZ; software, LW; validation, YH, JZ and GZ; formal analysis, BY; investigation, JZ; resources, LW; data curation, JZ; writing—original draft preparation, BY; writing—review and editing, BY; visualization, BY; supervision, BY; project administration, JZ; funding acquisition, BY. All authors have read and agreed to the published version of the manuscript.

Acknowledgments: TaiMei Baofa Cancer hospital (Dongping, Shandong Province, China, 271500).

Data availability statement: The data that support the findings of this study are available from [third party name] but restrictions apply to the availability of these data, which were used under license for the current study, and so are not publicly available. Data are, however, available from the authors upon reasonable request and with permission of [third party name], we will provide it.

Conflict of interest: The authors declare no conflict of interest.

References

1. Janeway CA, Travers P, Walport M, et al. The Humoral Immune Response. Garland Science. 2001.
2. Finn OJ. Immuno-oncology: understanding the function and dysfunction of the immune system in cancer. Annals of Oncology. 2012; 23: viii6-viii9. doi: 10.1093/annonc/mds256
3. Soman AD, Collins JM, DePetris G, et al. Isolated supraclavicular lymph node metastasis in pancreatic adenocarcinoma: a report of three cases and review of the literature. JOP. 2010; 11(6).
4. Heo CK, Bahk YY, Cho EW. Tumor-associated autoantibodies as diagnostic and prognostic biomarkers. BMB Reports. 2012; 45(12): 677–685. doi: 10.5483/bmbrep.2012.45.12.236
5. Sun G, Ye H, Wang X, et al. Autoantibodies against tumor-associated antigens combined with microRNAs in detecting esophageal squamous cell carcinoma. Cancer Medicine. 2019; 9(3): 1173–1182. doi: 10.1002/cam4.2792
6. Dudas SP, Chatterjee M, Tainsky MA. Usage of cancer associated autoantibodies in the detection of disease. Cancer Biomarkers. 2010; 6(5–6): 257–270. doi: 10.3233/cbm-2009-0138
7. Yu B, Han Y, Fu Q, et al. Awaken Immune Cells by Hapten Enhanced Intratumoral Chemotherapy with Penicillin Prolong Pancreatic Cancer Survival. Journal of Cancer. 2023; 14(8): 1282–1292. doi: 10.7150/jca.82985
8. Yu B, Zhang J, Fu Q, et al. Successful targeting in situ of an oncogenic nuclear antigen by hapten induced tumor associated autoantibodies (iTAA). Scientific Reports. 2023; 13(1). doi: 10.1038/s41598-023-36757-2

9. Gross BP, Wongrakpanich A, Francis MB, et al. A Therapeutic Microparticle-Based Tumor Lysate Vaccine Reduces Spontaneous Metastases in Murine Breast Cancer. The AAPS Journal. 2014; 16(6): 1194–1203. doi: 10.1208/s12248-014-9662-z
10. Diao L, Liu M. Rethinking Antigen Source: Cancer Vaccines Based on Whole Tumor Cell/tissue Lysate or Whole Tumor Cell. Advanced Science. 2023; 10(22): e2300121. doi: 10.1002/advs.202300121
11. Schnurr M, Galambos P, Scholz C, et al. Tumor cell lysate-pulsed human dendritic cells induce a T-cell response against pancreatic carcinoma cells: an in vitro model for the assessment of tumor vaccines. Cancer Res. 2001; 61(17): 6445–6450.
12. Lau SP, Klaase L, Vink M, et al. Autologous dendritic cells pulsed with allogeneic tumour cell lysate induce tumour-reactive T-cell responses in patients with pancreatic cancer: A phase I study. European Journal of Cancer. 2022; 169: 20–31. doi: 10.1016/j.ejca.2022.03.015
13. Dai L, Ren P, Liu M, et al. Using immunomic approach to enhance tumor-associated autoantibody detection in diagnosis of hepatocellular carcinoma. Clinical Immunology. 2014; 152(1-2): 127-139. doi: 10.1016/j.clim.2014.03.007
14. Tang ZM, Ling ZG, Wang CM, et al. Serum tumor-associated autoantibodies as diagnostic biomarkers for lung cancer: A systematic review and meta-analysis. Plos One. 2017; 12(7): e0182117. doi: 10.1371/journal.pone.0182117
15. Yu BF, Lu Y, Gao F, et al. Hapten-enhanced therapeutic effect in advanced stages of lung cancer by ultra-minimum incision personalized intratumoral chemoimmunotherapy therapy. Lung Cancer: Targets and Therapy. Published online January 2015: 1–11. doi: 10.2147/lctt.s70679
16. Kaminski JM, Shinohara E, Summers JB, et al. The controversial abscopal effect. Cancer Treatment Reviews. 2005; 31(3): 159–172. doi: 10.1016/j.ctrv.2005.03.004
17. Dai L, Peng XX, Tan EM, et al. Tumor-associated antigen CAPERα and microvessel density in hepatocellular carcinoma. Oncotarget. 2016; 7(13): 16985-16995. doi: 10.18632/oncotarget.7707
18. Im K, Mareninov S, Diaz MFP, et al. An Introduction to Performing Immunofluorescence Staining. Methods Mol. Biol. 2019: 299–311. doi: 10.1007/978-1-4939-8935-5
19. Yu BF., Chen D., Zhang J, et al. An Acute Inflammation with Special Expression of CD11 & CD4 Produces Abscopal Effect by Intramoral Injection Chemotherapy Drug with Hapten in Animal Model. Journal of Immunological Sciences. 2022; 6(3): 1-9. doi: 10.29245/2578-3009/2022/3.1236

Appendix